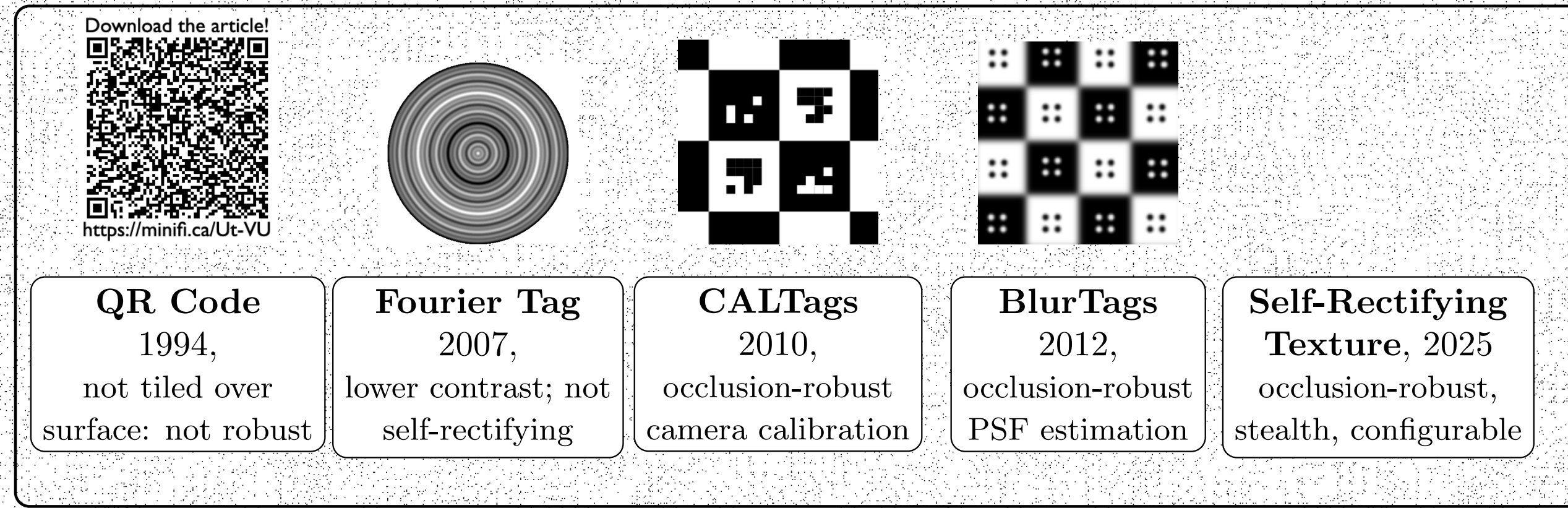


## Fiducial Markers for Product Traceability Applications

Traditional fiducial markers require high-contrast spatial landmarks for rectification. These are unsuitable for product traceability as they can be tampered.

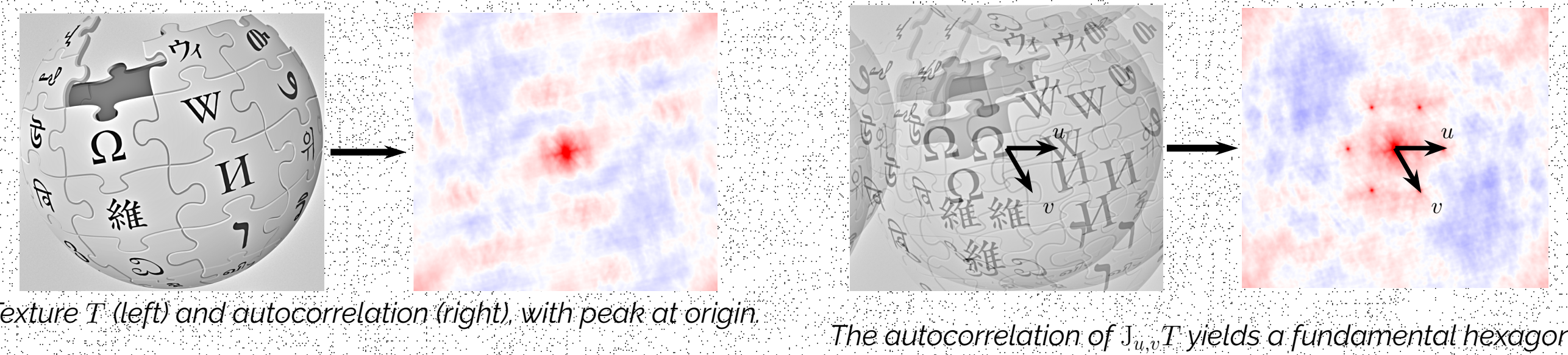


- We seek stealth markers that cover the entire surface, are robust to occlusion or intentional damage, and enable reliable complex surface rectification.

## Self-rectifying Textures Embed Landmarks in the Autocorrelation Domain

Instead of using spatial landmarks, we create landmarks in the autocorrelation domain by superimposing three copies of a texture  $T$  with relative shifts  $u$  and  $v$ . This is done by the operator  $J_{u,v}$ :

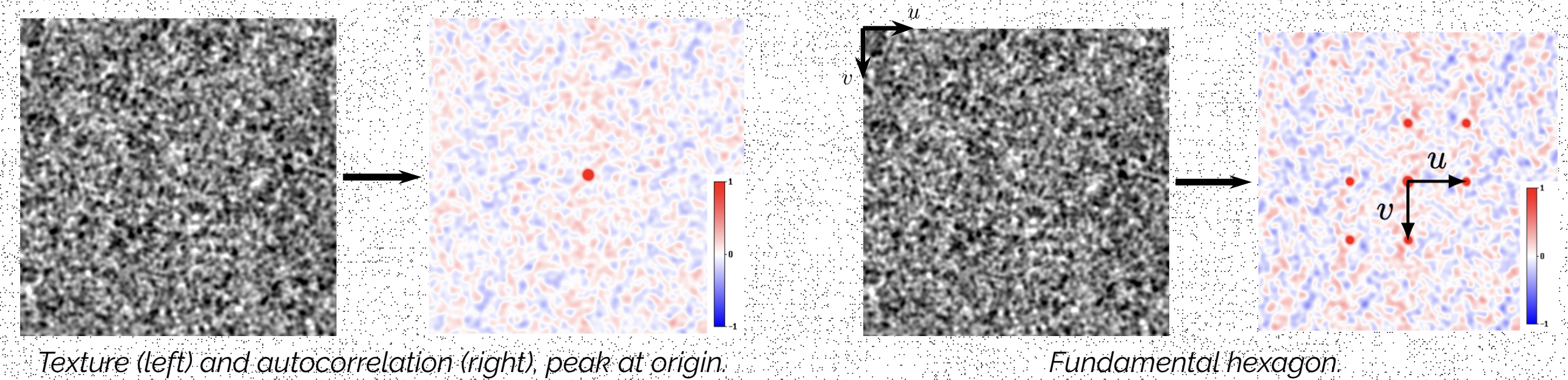
$$J_{u,v}T = T + T(\cdot - u) + T(\cdot - v).$$



Texture  $T$  (left) and autocorrelation (right), with peak at origin.

The autocorrelation of  $J_{u,v}T$  yields a fundamental hexagon.

Using subtle textures  $T$  (e.g., noise patterns or sparse point clouds) makes the superimposed copies  $J_{u,v}T$  suitable for repetition across a surface while preserving the landmarks (autocorrelation peak locations). Importantly their superposition remains imperceptible to the naked eye.



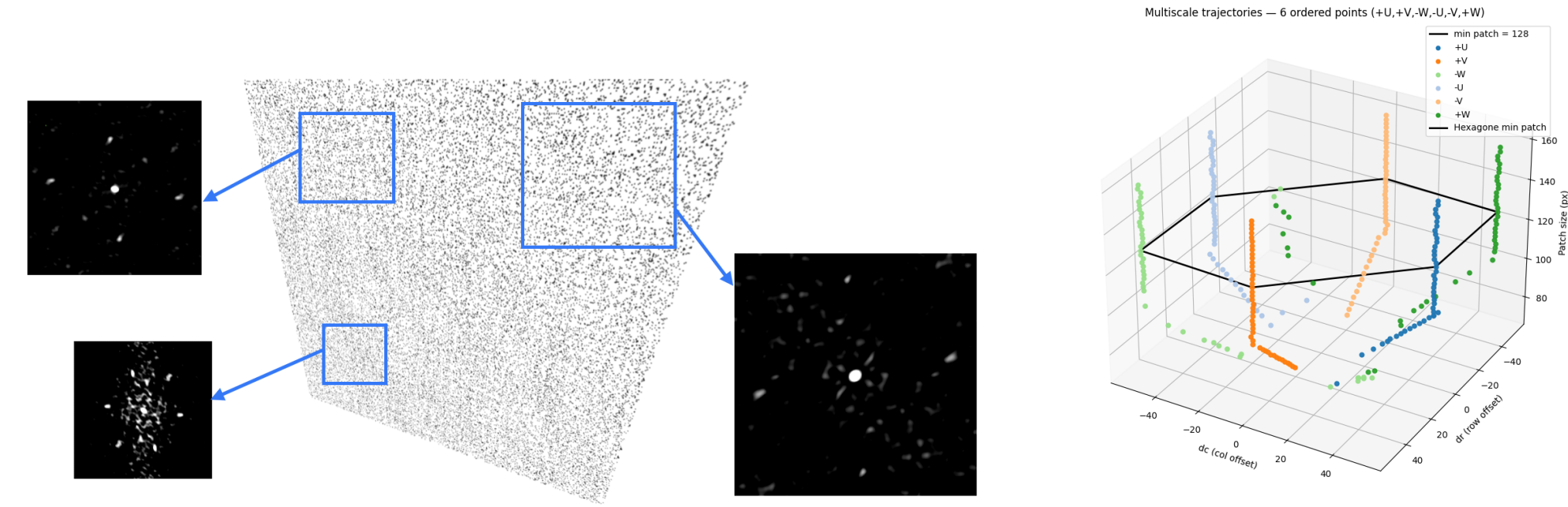
Texture (left) and autocorrelation (right), peak at origin.

Fundamental hexagon.

## Local hexagon $\Rightarrow$ Affine $A_i \Rightarrow$ Global $H$

### Autocorrelation and Sub-pixel peak detection

Illustration of a self-rectifying texture  $J_{u,v}T$  subject to a homographic deformation  $H$ . We recover the distortion by estimating the corresponding homography from the detected autocorrelation peaks  $(u, v)$ .



The two peaks  $u$  and  $v$  defining the hexagon in the autocorrelation  $R$  of each patch are refined simultaneously to obtain sub-pixel accuracy. Selecting the best pair with energy maximization gives the fundamental hexagon that maximizes the autocorrelation and the corresponding minimal stable patch  $P_i$  where  $u_{fin}$  and  $v_{fin}$  still stable:

$$(u_{fin}, v_{fin}) = \underset{u \neq v \in \mathcal{P}}{\operatorname{argmax}} 2(\bar{R}(u) + \bar{R}(v) + \bar{R}(u - v)).$$

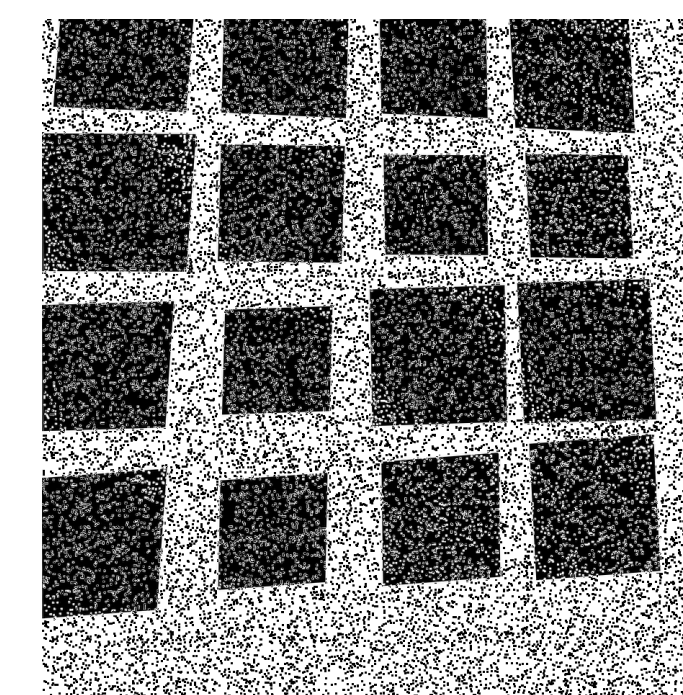
### Local Observation and Patchwise rectification

We estimate the differential  $A_i = \nabla_{H^{-1}(y_i)}H$  of the deformation  $H$  using the fundamental hexagon. Given the texture  $J_{u,v}T$ , we use phase correlation between  $J_{u,v}T$  and local minimal stable patch  $P_i$  to estimate the translation:

$$b_i = \underset{\tau \in \mathbb{R}^2}{\operatorname{argmax}} \mathcal{F}^{-1} \left( \frac{\widehat{J_{u,v}T}(\omega) \overline{\widehat{P_i}(\omega)}}{\widehat{J_{u,v}T}(\omega) \widehat{P_i}(\omega)} \right) (\tau).$$

The first-order Taylor approximation of  $H$  around  $H^{-1}(y_i) = A_i^{-1}(y_i - b_i)$  is:  $h \mapsto A_i h + b_i$ . Its inverse, which rectifies the patch around  $y_i$ , is

$$h \mapsto A_i^{-1}(h - b_i)$$



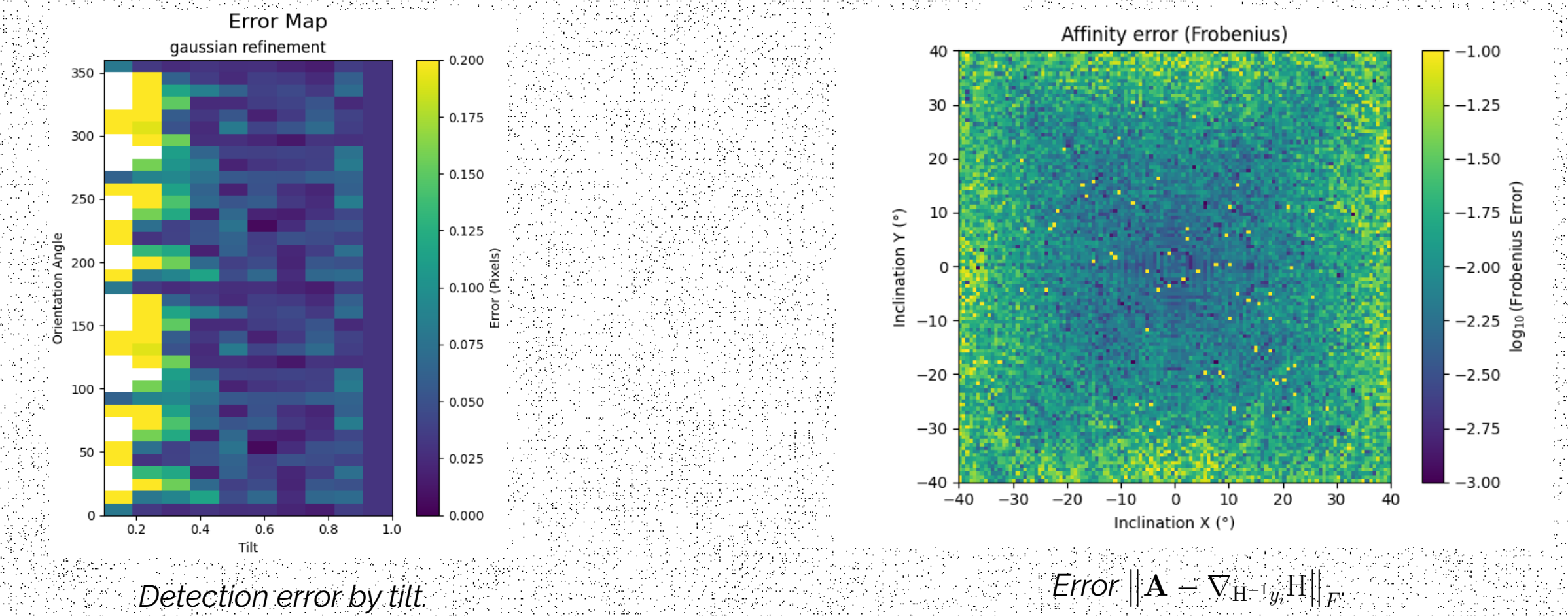
### Homography estimation (modulo translation)

Seek a homography  $H \in \operatorname{PGL}(3, \mathbb{R}) \cong \operatorname{SL}(3, \mathbb{R})$  whose differentials match the observed matrices  $A_i$  in  $y_i$ .

$$H^* = \underset{H \in \mathcal{H}}{\operatorname{argmin}} \frac{1}{n} \sum_{i=1}^n \|\nabla_{H^{-1}(y_i)}H - A_i\|_F.$$

## Peak detection, inclination angles and occlusion

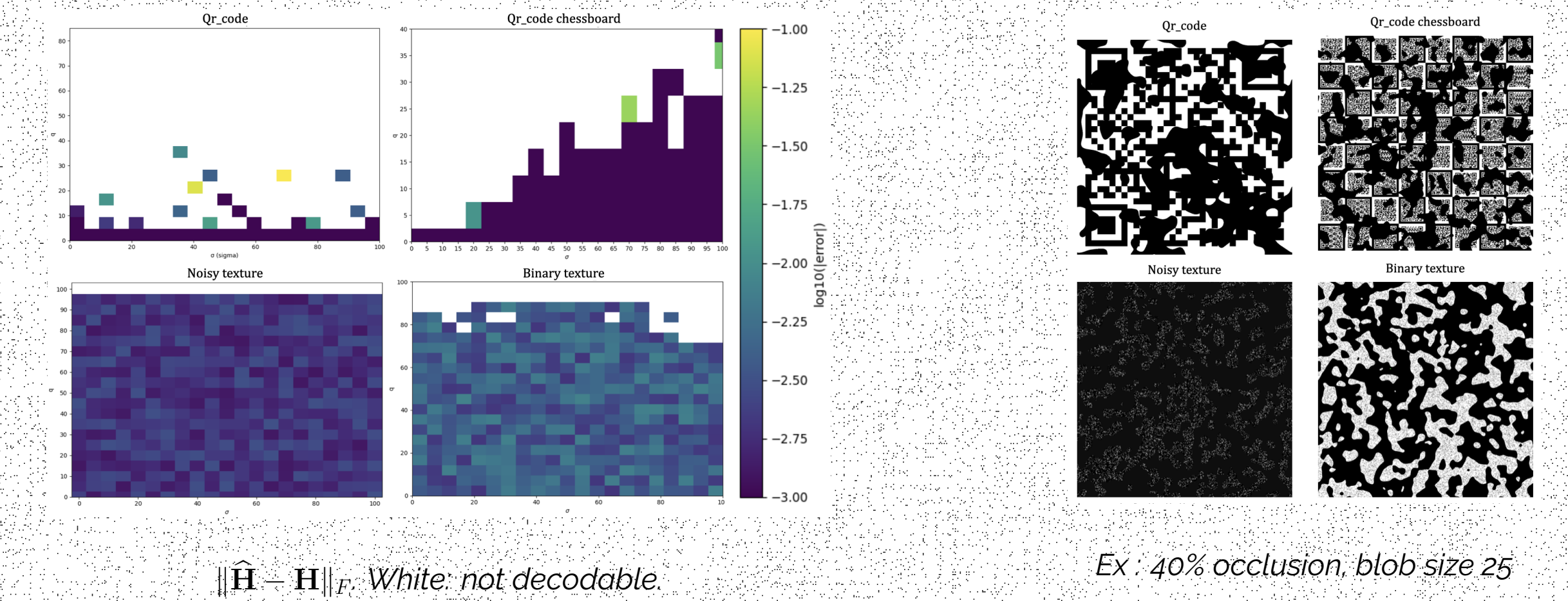
The first image shows sub-pixel peak detection accuracy, when faced with different tilt deformations oriented at different angles in the affine model:  $A = \lambda R_{-\theta} \begin{bmatrix} \tilde{t} & 0 \\ 0 & 1 \end{bmatrix} R_{\theta} R_{\psi}$  encodes scale  $\lambda$ , rotation  $\theta$ , tilt  $\tilde{t}$ , and its orientation  $\psi$ . Leading to precise local affinity estimation and accurate recovery of the overall deformation.



Detection error by tilt.

Error  $\|A - \nabla_{H^{-1}(y_i)}H\|_F$ .

Landmarks in autocorrelation are robust to occlusion, unlike spatial landmarks, which can be easily destroyed.



$\|\hat{H} - H\|_F$ . White: not decodable.

Ex : 40% occlusion, blob size 25

## Conclusion

Autocorrelation-based textures provide robust, landmark-free rectification from a single image. Their stealth design ensures resilience to occlusion and tampering thanks to the requirement to know the initial shifts and basic texture, thus enabling reliable geometric recovery for large-scale traceability.

## References

Hara, Masahiro and Watabe (1998). *Optically readable two-dimensional code and method and apparatus using the same*.  
Olson, Edwin (2011). "AprilTag: A robust and flexible visual fiducial system". In: IEEE.